JOURNAL OF THE FACULTY OF ENGINEERING, THE UNIVERSITY OF TOKYO (B) 1
Vol. 38, No. 4 (1986), PP. 1~18

MHD Flow in Liquid Metal Blankets with Helical Vanes

by

Haruki MADARAME* and Mark S. TILLACK**

(Received April 2, 1986)

MHD flow in liquid metal blankets with helical vanes is discussed. The velocity profile and the MHD pressure drop in a pipe with a diametric turning vane under an axial magnetic field are derived with the assumption of fully developed conditions. The fluid flows helically along the vane with the velocity almost inversely proportional to the radius. Eddy currents flow radially in the fluid and then back through the outer wall and the vane. The radial current and the axial field cause a force in the circumferential direction, which resists the circumferential flow. Since the current intensity can be reduced by thinning the vane, the MHD pressure drop is low in a pipe with a thin vane.

A reference design of a liquid metal blanket with a helical vane is made, and the required thickness of the vane is discussed from the viewpoint of structural strength. The temperature distribution is calculated and is compared with those of pipes without vanes. The vane is shown to keep the first wall temperature low with a small additional pressure drop.

1. Introduction

In self-cooled liquid metal blankets, the liquid metal serves as both breeder and coolant. Heat transfer requirements seem to be reduced because most of the nuclear heating is deposited directly in the breeder-coolant. But the bulk heating rate is high in the first wall, which also receives radiation heat from the plasma. Although a liquid metal has a high thermal conductivity, good heat transfer cannot be expected in a magnetic field if the coolant does not mix and the heat is transmitted radially only by heat conduction. The temperature difference in the radial direction may be very large unless the pipe diameter is kept small.

Because of the low heat capacity of the coolant, the bulk coolant temperature rises quickly unless the coolant velocity is high. However, the velocity must be kept low in a magnetic field in order to maintain the MHD pressure drop within acceptable limits. It is not desirable to use a great number of short pipes because the configuration of the blanket becomes complicated. A single large pipe with a helical vane has the advantage of both large thermal capacity and good heat transfer. As the vane supplies a relatively cool liquid metal to the first wall, the first wall temperature is kept low even if the pipe is thick and long. However, the existence of a helical vane causes an additional pressure drop. In this report, merits and demerits of helical pipes in a fusion reactor blanket are discussed.

* Department of Nuclear Engineering

** School of Engineering and Applied Science, University of California, Los Angeles

Liquid metal flow under strong magnetic fields has been studied by many researchers both theoretically and experimentally. The recent advances in MHD duct flow studies were summarized by Hunt and Holroyd[1]. In this report, we deal with one particular MHD duct flow problem. Since the passage of fluid in a pipe with a helical vane has a peculiar configuration, an interesting velocity profile appears.

2. MHD Pressure Drop

2.1 Calculational Model and Assumptions

Consider a liquid metal flowing in a pipe with radius R, as shown in Fig. 1. The pipe has wall thickness t_w, and a diametric turning vane of thickness t_v and helical pitch L_p. The electrical conductivity of the wall and the vane is σ_w while that of the liquid is σ_f. The density and the viscosity of the liquid are ρ and η, respectively. The liquid has an average velocity w_b in the axial direction (z-axis) which is parallel to the imposed magnetic field. The radial and circumferential components of the velocity are denoted by u and v, respectively, as shown in Fig. 2.

The magnetic field is assumed to be very strong so that the conditions of Ha $\gg$ 1 and N $\gg$ 1 are satisfied, where Ha $= BR\sqrt{\sigma_f/\eta}$ is the Hartmann number and N $= B^2R\sigma_f/\rho w_b$ is the interaction parameter. The pipe wall and the vane are assumed to be thin ($\phi_w = \sigma_w t_w/\sigma_f R \ll 1$, $\phi_v = \sigma_w t_v/\sigma_f R \ll 1$). The magnetic Reynolds number is assumed to be small, hence the induced field can be neglected. These conditions are normally satisfied in a fusion blanket.

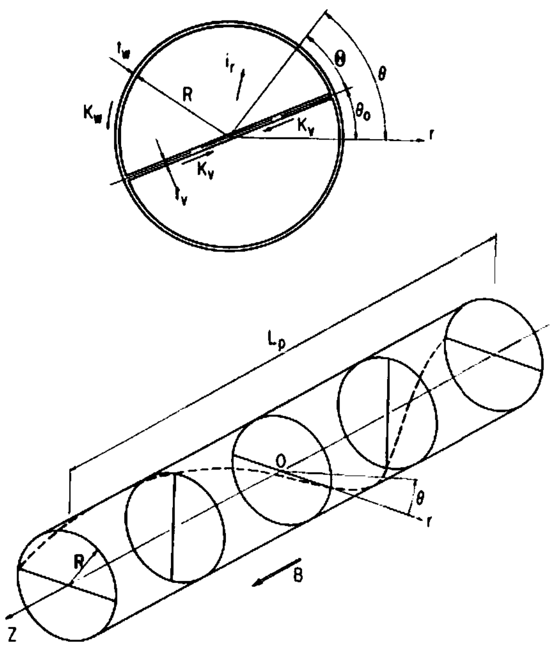

Fig. 1. Calculational model

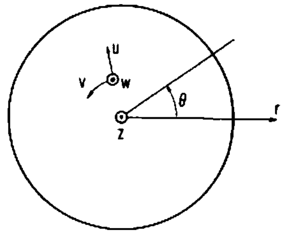

Fig. 2. Coordinate system

No electromagnetic force arises in the z direction, since the magnetic field is parallel to the z-axis. The turning vane generates helical flow, which induces radial currents in the fluid. The radial current and the axial magnetic field cause a force in the circumferential direction, which resists the circumferential flow. The MHD pressure drop in the pipe is caused not by an axial force but by a circumferential force. In the following, the electric current and fluid flow distributions are studied, and then the MHD pressure drop is calculated.

If the angular position of the vane is given by

$$\theta_o = 2\pi \frac{z}{L_p} \tag{1}$$

then the angular distance from the vane is

$$\Theta = \theta - \theta_o \tag{2}$$

The flow is assumed to be fully developed. In other words, the velocity profile is constant in a coordinate system moving with the vane. As there is no electromotive force in the magnetic field direction in the pipe, the potential does not change in the z direction unless there is an external source. In order to solve for the MHD pressure drop and flow distribution, the eddy current and electric potential distributions must be solved using basic equations which are discussed later. In this geometry, due in large part to the assumption of fully developed conditions, simplifications can be made to allow a direct analytic solution.

The flow passage in the pipe with a helical vane shown in Fig. 3a is surrounded by a wall parallel to the field lines (the outer wall) and a wall which cuts the field lines (the turning vane), similar to the rectangular duct shown in Fig. 3b. The following three kinds of regions appear in rectangular duct flow[2),3)]:

1) core region
2) primary, or Hartmann boundary layers on the walls which cut the field lines
3) secondary boundary layers on the walls parallel to the field lines

In analogy with rectangular duct flow, pipe flow with a vane is considered to be composed of a core region, a Hartmann layer on the vane, and a secondary boundary layer on the outer wall, as is shown in Fig. 3a. The thickness of the Hartmann layer is proportional to the normal component of the magnetic field. In this report, the Hartmann layer is assumed to be thin because of a very strong magnetic field. Since the vane is nearly parallel to the magnetic field lines in the neighborhood of $r = 0$, this assumption may not be valid there. However, the assumption is valid away from the point $r = 0$ in the extreme case when the magnetic field strength is infinite and the point is occupied not by the boundary layer, but by the vane. The assumption of a thin Hartmann layer on the vane is a proper method to get a perspective solution of this MHD flow problem, though the limit in applicability of the solution should be examined. This is a subject for future study.

Since there is a normal component of magnetic field in the thin Hartmann layer, the flow quantity in the Hartmann layer is assumed to be negligible and to have no effect on the core

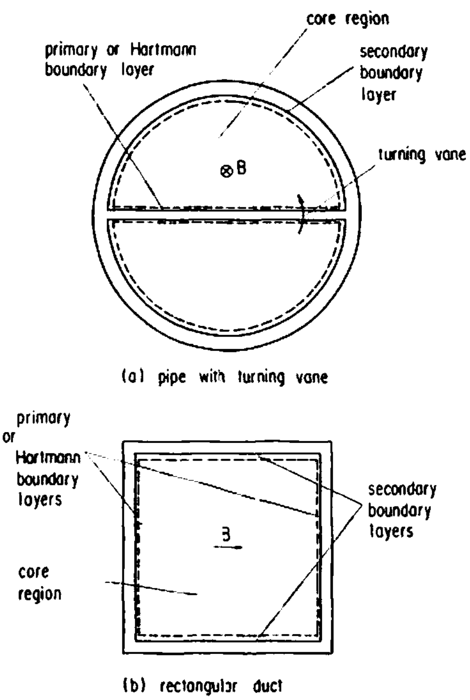

Fig. 3. Different kinds of regions in MHD duct flow

flow. The thickness of the secondary boundary layer is proportional to $Ha^{-1/2}$, which is thin when the magnetic field is very strong. Both the Hartmann and secondary boundary layers can carry an electric current in addition to the vane and the outer wall. The resistivity of these layers is inversely proportional to their thickness, hence the current in them is small compared with that in the vane and the outer wall when the boundary layers are very thin. The current in the boundary layers is assumed to be negligible. The flow quantity in the secondary boundary layer on the outer wall may be considerable, as in the case of a rectangular duct.

2.2 *Basic Equations and Eddy Current Distribution*

The magnetohydrodynamic equations for steady incompressible flow are:

$$\rho(V\cdot\nabla)V = -\nabla p + j\times B + \eta\nabla^2 V \tag{3}$$

$$\nabla\cdot V = 0 \tag{4}$$

$$j = \sigma_f(\nabla\Phi + V\times B) \tag{5}$$

$$\nabla\cdot J = 0 \tag{6}$$

where $V\,(u, v, w)$, p, $j\,(j_r, j_\theta, j_z)$ and Φ are velocity, pressure, current density and electric potential, respectively. The magnetic flux density is equal to the imposed magnetic field $B\,(0, 0, B)$, since the magnetic Reynolds number is small and the induced field can be neglected. Equation (3) can be non-dimensionalized with respect to B, R, and w_b as follows:

$$N^{-1}(V'\cdot\nabla')V' = -\nabla'p' + j' \times B' + \mathrm{Ha}^{-2}\nabla'^2 V' \tag{7}$$

Since N >> 1 and Ha >> 1, the first and last terms are negligible, except in boundary layers or free shear layers, where large gradients and/or large velocities make these terms significant. Therefore, in the core region,

$$\nabla'p' = j' \times B' \tag{8}$$

or

$$\nabla p = j \times B \tag{9}$$

Taking the curl of eq. (9), we obtain:

$$\frac{\partial j_r}{\partial z} = 0 \tag{10}$$

$$\frac{\partial j_\theta}{\partial z} = 0 \tag{11}$$

$$\frac{1}{r}\frac{\partial}{\partial r}(rj_r) + \frac{1}{r}\frac{\partial j_\theta}{\partial \theta} = 0 \tag{12}$$

The current distributions in any r-Θ planes are the same, because the flow is fully developed. Since the radial and circumferential currents are uniform both in the axial direction [eqs. (10) and (11)] and in the direction defined by the vane joint (where Θ is a function of z), they must also be uniform in the circumferential direction. Thus:

$$\frac{\partial j_r}{\partial \theta} = 0 \tag{13}$$

$$\frac{\partial j_\theta}{\partial \theta} = 0 \tag{14}$$

From eqs. (12) and (14), we obtain:

$$\frac{\partial}{\partial r}(rj_r) = 0 \tag{15}$$

Substituting eqs. (14) and (15) into eq. (6), we obtain:

$$\frac{\partial j_z}{\partial z} = 0 \tag{16}$$

Using eq. (16) and the z-component of eq. (5), we obtain the following relation:

$$\frac{\partial \Phi}{\partial z} = \text{constant}, \tag{17}$$

which means that the potential is uniform in the z direction. Analogous to the derivation of the current density, $\partial\Phi/\partial\Theta$ must also be constant to satisfy eq. (17) under fully developed conditions.

There is no electromotive force in the vane. From this fact and the periodic boundary condition, the electric potentials in the fluid at $\Theta = 0$ and $\Theta = \pi$ are the same. Thus:

$$\frac{\partial\Phi}{\partial\Theta} = 0 \tag{18}$$

and again, fully developed conditions lead to:

$$\frac{\partial\Phi}{\partial z} = 0 \tag{19}$$

$$\frac{\partial\Phi}{\partial\theta} = 0 \tag{20}$$

In the core region of the flow, eq. (19) and the z-component of eq. (5) lead to:

$$j_z = 0 \tag{21}$$

Therefore, there is no z-directional current.

Conservation of mass can be expressed in the form of a mass balance in a thin disk of radius r and height dz:

$$r\int_0^\pi u(r, \Theta)\,d\Theta + \frac{\partial}{\partial z}\int_0^\pi\int_0^r w(r', \Theta)\,r'\,d\Theta\,dr' = 0 \tag{22}$$

Since the flow is fully developed, the second term is zero, thus:

$$r\int_0^\pi u(r, \Theta)\,d\Theta = 0 \tag{23}$$

From eq. (20) and the θ-component of eq. (5), we obtain:

$$j_\theta = -\sigma_f u B \tag{24}$$

Differentiating the above equation with respect to θ and substituting eq. (14), we obtain:

$$\frac{\partial u}{\partial\theta} = 0 \tag{25}$$

which implies:

$$\frac{\partial u}{\partial\Theta} = 0 \tag{26}$$

Therefore, eq. (23) can be rewritten as follows:

$$\pi r u(r) = 0 \tag{27}$$

which means that the radial velocity component is zero everywhere. Substituting eq. (27) into eq. (24), we obtain:

$$j_\theta \equiv 0 \tag{28}$$

Thus the axial and circumferential components of the current in the core region of the flow are zero. The radial component of the current changes only in the radial direction and satisfies eq. (15).

2.3 *Electric Potential Distribution*

In the previous section, the spatial distribution of the current in the fluid was obtained. In order to know the current intensity, we need the potential distribution, which is determined by the resistance in the vane and the outer wall.

From eqs. (5), (13), and (20), we obtain:

$$\frac{\partial v}{\partial \theta} = 0 \tag{29}$$

Substituting eqs. (27) and (29) into eq. (4), we obtain:

$$\frac{\partial w}{\partial z} = 0 \tag{30}$$

and again fully developed conditions lead to:

$$\frac{\partial w}{\partial \theta} = 0 \tag{31}$$

On the surface of the vane, the normal component of the velocity is zero, thus:

$$v(r) = \frac{2\pi}{L_p} r w(r) \tag{32}$$

which holds regardless of the value of Θ.

Equation (5) can be rewritten as follows:

$$\frac{d\Phi}{dr} = vB - \frac{j_r}{\sigma_f} \tag{33}$$

The radial current in the core region can be assumed to return entirely through the vane. If the current in the vane per unit length in the z direction is represented by K_v, then the conservation of current is given by:

$$K_v = \pi r j_r \tag{34}$$

Substituting eqs. (32) and (34) into eq. (33), we obtain:

$$\frac{d\Phi}{dr} = \frac{2\pi B}{L_p} rw(r) - \frac{K_v}{\pi \sigma_f} \frac{1}{r} \tag{35}$$

The above equation gives the electric potential in the fluid. Since there is no electromotive force in the vane, the electric potential in the vane is given by:

$$\frac{d\Phi}{dr} = \frac{K_v}{\sigma_w t_v} \tag{36}$$

The electric potentials in the fluid and in the vane must match, thus:

$$w(r) = \frac{L_p}{2\pi B} \frac{1}{\sigma_w t_v} \frac{1}{r} (1 + \frac{\phi_v R}{\pi r}) K_v \tag{37}$$

$$\Phi(r) = \frac{r}{\sigma_w t_v} K_v \tag{38}$$

where the electric potential at $r = 0$ was assumed to be zero.

Figure 4 shows the outer wall of the pipe. Electric current flows spirally in the wall to the joint of the vane, which induces an electric potential in the outer wall. Since j_r is constant at $r = R$, the current density in the wall is zero at $\Theta = \pi/2$ and varies linearly with Θ:

$$K_w(\Theta) = Sj_r(R) (\frac{2\Theta}{\pi} - 1) = \frac{S}{\pi R} (\frac{2\Theta}{\pi} - 1) K_v \tag{39}$$

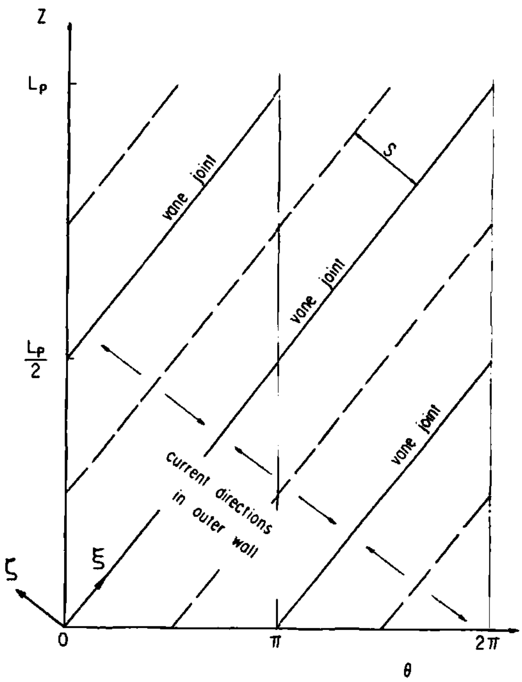

Fig. 4. Current direction in outer wall

in the direction of the unit vector

$$\vec{\ell} = \frac{L_p \vec{\Theta} + 2\pi R \vec{z}}{\{L_p^2 + (2\pi R)^2\}^{1/2}} \qquad (40)$$

where

$$S = \frac{\pi R L_p}{2\{L_p^2 + (2\pi R)^2\}^{1/2}} \qquad (41)$$

The electric potential in the pipe wall is calculated by integrating the current density:

$$\Phi_w(\Theta) - \Phi_w(0) = \frac{2S^2}{\pi \sigma_w t_w R} K_v \frac{\Theta}{\pi}(1 - \frac{\Theta}{\pi}) \qquad (42)$$

where $\Phi_w(0) = RK_v/\sigma_w t_w$ is the potential at the joint of the vane. The electric potential in the wall is different from that in the core liquid. This difference is compensated by an electromotive force in the boundary layer near the wall.

2.4 *Current Intensity*

Equations (29) and (31) do not hold in the boundary layer on the outer wall where viscous forces are not negligible. The layer is thin, and the radial velocity component is zero both on the outer wall surface and in the core. Therefore, the radial velocity component can be neglected in the layer. Consider a coordinate system in the boundary layer consisting of the ξ coordinate axis, which is parallel to the joint in the vane, and the ζ coordinate axis, which is perpendicular to the ξ axis (as shown in Fig. 4). The continuity equation in the layer is as follows:

$$\frac{du_\xi}{d\xi} + \frac{du_\zeta}{d\zeta} = 0 \qquad (43)$$

where u_ξ and u_ζ are velocity components in the ξ and ζ direction, respectively. Fully developed conditions lead to $\partial/\partial\xi = 0$, thus:

$$\frac{du_\zeta}{d\zeta} = 0 \qquad (44)$$

At the joint of the vane ($\zeta = 0$), $u_\zeta = 0$, hence the velocity component perpendicular to the joint, u_ζ, is zero everywhere. Therefore, eq. (32) holds in the boundary layer on the outer wall as well as in the core region.

If the boundary layer thickness is represented by δ, then the following relation is necessary such that the electromotive force in the boundary layer compensates the potential difference between the core fluid at $r = R$ and the outer wall:

$$\Phi_w(\Theta) - \Phi_w(0) = \int_{R-\delta}^{R} \nu B \, dr = \int_{R-\delta}^{R} \frac{2\pi B r}{L_p} w \, dr$$
$$= \frac{2S^2}{\pi \sigma_w t_w R} \frac{\Theta}{\pi} \left(1 - \frac{\Theta}{\pi}\right) K_v \tag{45}$$

Integrating eq. (45) from $\Theta = 0$ to $\Theta = \pi$ and defining the boundary layer flow quantity in one half period of the vane as: $Q_{B.L.} = \int_{R-\delta}^{R} \int_0^{\pi} wR \, d\, r d\Theta$, we obtain:

$$Q_{B.L.} = \frac{L_p S^2}{6\pi \sigma_w B t_w R} K_v \tag{46}$$

The flow quantity in the core region is given as follows:

$$Q_{core} = Q_{total} - Q_{B.L.} = \frac{\pi}{2} R^2 w_b - \frac{L_p S^2}{6\pi \sigma_w B t_w R} K_v \tag{47}$$

where w_b is the average velocity in the pipe in the z direction.

The integral of eq. (37) in the core region also gives the core flow quantity. Thus:

$$Q_{core} = \int_{r_o}^{R} \frac{L_p}{2\pi B} \frac{1}{\sigma_w t_w} \frac{1}{r} \left(1 + \frac{\phi_v R}{\pi r}\right) K_v \, \pi r dr$$
$$= \frac{L_p R K_v}{2\sigma_w B t_v} \left\{1 - \epsilon - \frac{\phi_v}{\pi} \ln \epsilon\right\} \tag{48}$$

where $\epsilon = r_o/R$. The value of w obtained from eq. (37) approaches infinity as r tends to zero. The vane was assumed to be very thin. But in the neighborhood of $r = 0$, the finite thickness affects the velocity profile. The vane occupies the region $r \leqq t_v/2$ when $\Theta = \pi/2$. When $\Theta \neq \pi/2$, the vane occupies a larger region. In eq. (32), r_o is the average inner radius of the core region. It is larger than $t_v/2$, but still on the average very small compared with R. When $\epsilon << 1$, the following relations can be used to simplify eq. (48):

$$\frac{t_v}{2R} \ln \epsilon < \epsilon \ln \epsilon << 1 \tag{49}$$

Eliminating the negligible terms from eq. (48), we obtain:

$$Q_{core} = \frac{L_p R K_v}{2\sigma_w B t_v} \tag{50}$$

Substituting eq. (50) into eq. (47) and arranging, the current in the vane is obtained as follows:

$$K_v = \frac{\pi \sigma_w B R t_v w_b / L_p}{1 + S^2 t_v / 3\pi t_w R^2} \tag{51}$$

The radial current in the core liquid is given by:

$$j_r = \frac{\sigma_w B R t_v w_b / L_p}{1 + S^2 t_v / 3\pi t_w R^2} \frac{1}{r} \tag{52}$$

2.5 *MHD Pressure Drop and Velocity Profile*

The magnetic field is parallel to the z-axis. From eq. (9), we obtain:

$$\frac{\partial p}{\partial z} = 0 \tag{53}$$

which means that the pressure is uniform in the z direction. The pressure is not uniform in an r-θ plane but distributes in the following manner:

$$\frac{\partial p}{\partial \theta} = B j_r \tag{54}$$

Equations (13) and (14) were derived from eqs. (10) and (11) with the assumption of fully developed conditions. Although $\partial p/\partial z = 0$, $\partial p/\partial \theta$ is not zero, since the pressure p is a linear function of z as well as of Θ even in a fully developed flow. The flow in the pipe has a circumferential component, v, which was written in eq. (32). The radial current and the axial magnetic field cause a force in the circumferential direction, which resists the flow. The MHD pressure drop is given as follows:

$$-\frac{dp}{dz} = \frac{2\pi r}{L_p} B j_r = \sigma_f B^2 w_b \frac{2\pi R^2}{L_p{}^2} \frac{\phi_v}{1 + S^2 t_v / 3\pi t_w R^2} \tag{55}$$

where the differentiation d/dz is done in the direction of the fluid particle path. The above equation gives a decreasing rate of the average pressure in an r-θ plane in the z direction. The velocity profile in the core region is obtained by substituting eq. (51) into eq. (37):

$$w = \frac{w_b}{2} \frac{R}{r} \frac{1 + \phi_v R/\pi r}{1 + S^2 t_v / 3\pi t_w R^2} \tag{56}$$

The flow quantity in the wall jet is given by:

$$\int_{R-\delta}^{R} w dr = \frac{w_b S t_v}{2 t_w} \frac{1}{1 + S^2 t_v / 3\pi t_w R^2} \frac{\Theta}{\pi} \left(1 - \frac{\Theta}{\pi}\right) \tag{57}$$

A schematic view of the velocity distribution is shown in Fig. 5.

As is obvious from eq. (55), the MHD pressure drop can be reduced by thinning the vane. The velocity profile is approximately proportional to $1/r$ in the core region, and becomes nearly $w_b/2$ when $r = R$. The turning vane not only causes the flow to swirl, but also makes the velocity near the wall high (as compared to fully developed parallel flow without the vane).

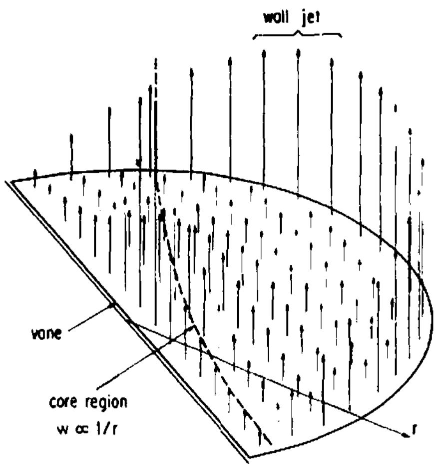

Fig. 5. Schematic view of velocity distribution

3. Reference Design of a Blanket Using Helical Vanes

3.1 *Purpose of Design and Design Parameters*

Liquid metal blankets must satisfy several requirements. The wall temperature must be within an allowable range, which is difficult to attain without good heat transfer. The MHD pressure drop must be low so that the wall can withstand the internal pressure. Helical vanes in blankets may increase not only the heat transfer coefficient, but also the MHD pressure drop. In order to clarify overall merits and demerits of helical vanes, a reference design is made using the parameters shown in Table 1. For simplicity, the pipe wall is assumed to be an ideal conductor. In this case, the MHD pressure drop is given as follows:

$$-\frac{dp}{dz} = \sigma_f B^2 w_b \frac{2\pi R^2}{L_p^2} \phi_v \tag{58}$$

The flow quantity in the wall jet decreases with increasing outer wall conductivity as can be calculated by eq. (57). Thus, the existence of a wall jet is neglected in the following.

3.2 *MHD Pressure Drop and Stress in Vane*

The MHD pressure drop can be reduced by thinning the vane. But the stress in the vane increases with decreasing thickness. The vane must be thick enough to withstand the electromagnetic load induced by the current in the vane and the pressure difference on both sides of the vane. Figure 6 shows the distributions of the loads in a cross-section of the vane. The intensity of the electromagnetic load is uniformly $K_v B$, but the direction of the load is reversed at the center, since the current direction is reversed. The pressure distribution in each channel can be obtained by eqs. (9), (15), (21), and (28). The pressure changes only in the circumferential direction as follows:

Table 1. Parameters of Reference Blanket

Pipe Length	L	2 m
Helical Pitch of Turning Vane	L_p	2 m
Pipe Radius	R	5 cm
Vane Thickness	t_v	0.5 mm
Bulk Velocity of Coolant	w_b	0.3 m/s
Magnetic Field Strength	B	7.5 T
Conductivity of Coolant	σ_f	3.0 MS/m
Conductivity of Wall	σ_w	1.5 MS/m
Density of Coolant	ρ	490 kg/m^3
Specific Heat of Coolant	c_p	4.2 kJ/kg·K
Thermal Conductivity of Coolant	k	48.4 W/m·K
Surface Heat Load	q_o''	0.75 MW/m^2
Average Heat Generation in Coolant	$\overline{q}'''$	11.45 MW/m^3
Inlet Coolant Temperature	T_{in}	225°C
Bulk Coolant Temperature at Outlet	T_{out}	293°C
Maximum Interface Temperature	T_{max}	453°C
MHD Pressure Drop	Δp	2.0 kPa
Maximum Stress in Vane	σ_{max}	20 MPa

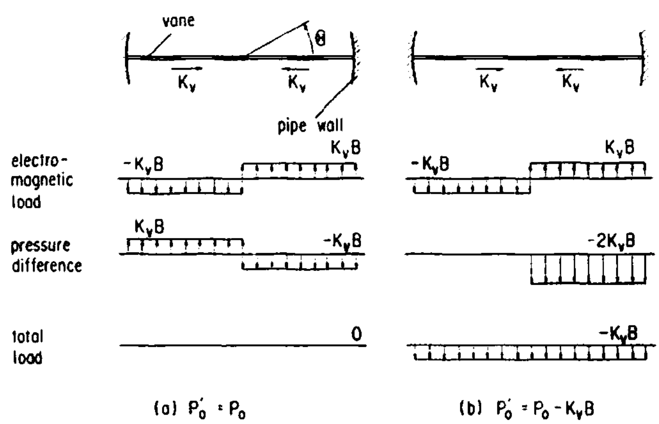

Fig. 6. Distribution of loads

$$p = p_o - \frac{K_v B \Theta}{\pi} \qquad (0 < \Theta < \pi) \tag{59}$$

$$p = p_o' - \frac{K_v B(\Theta - \pi)}{\pi} \qquad (\pi < \Theta < 2\pi) \tag{60}$$

where p_o and p_o' are determined by the inlet or outlet condition. If the average pressure in each channel in the same cross-section is the same, then $p_o' = p_o$, and the pressure difference is distributed as shown in Fig. 6a. In this case, the pressure difference cancels the electromotive load, and the total load is zero everywhere. This is the optimum condition. However, the average pressure in each channel is not necessarily the same. As an example, p_o' is assumed to be equal to $p_o - K_v B$ in the following. In this case, the pressure difference is zero at $\Theta = \pi$ and is $2K_v B$ at $\Theta = 0$ ($\Theta = 2\pi$). The total load is uniformly $K_v B$ as shown in Fig. 6b. The maximum bending moment appears at both fixed ends and is given as follows:

$$M_{max} = \frac{1}{3} K_v B R^2 \tag{61}$$

The maximum stress is given by:

$$\sigma_{max} = 2K_v B R^2 / t_v^2 \tag{62}$$

The current in the vane in the case with a perfectly conducting outer pipe wall is given as follows:

$$K_v = \sigma_f B w_b \frac{\pi R^2}{L_p} \phi_v \tag{63}$$

Using the parameters in Table 1, the maximum stress is calculated to be 20 MPa, which is considered to be within an allowable range.

The MHD pressure gradient is calculated by eq. (58) to be 1.0 kPa/m. The MHD pressure drop in the pipe is only 2.0 kPa. The increase in the total blanket pressure due to the vane is insignificant.

3.3 Temperature Distribution

The purpose of helical vanes is to make the temperature distribution in the coolant uniform. The temperature distribution at the outlet of the pipe with a helical vane is compared with those in the pipes without a vane. In the pipe with a vane, the vane conductivity, ϕ_v, and the wall thickness ratio, t_v/t_w, are assumed sufficiently small such that the velocity distribution eq. (56) may be simplified to:

$$w = \frac{w_b}{2} \frac{R}{r} \tag{64}$$

Parabolic and slug flow velocity profiles are assumed in the pipes without a vane. In each case, the temperature is calculated using a finite difference method on the energy equation:

$$\frac{\partial T}{\partial z} = \frac{k}{\rho c_p w(r)} \left\{ \frac{1}{r} \frac{\partial}{\partial r} \left(r \frac{\partial T}{\partial r} \right) + \frac{1}{r^2} \frac{\partial^2 T}{\partial \theta^2} \right\} + \frac{q'''}{\rho c_p w(r)} \tag{65}$$

where k is the thermal conductivity, ρ is the density and c_p is the specific heat of the coolant.

The following equation is used for the heat generation rate in the coolant:

$$q''' = q_o''' \exp(-x/s) \tag{66}$$

where $s = 0.15$ m. $q_o''' = 15$ MW/m^3, and x is the distance from the nearest point to the plasma as shown in Fig. 7. The heat flux on the cooling surface of the pipe is assumed to be given as follows:

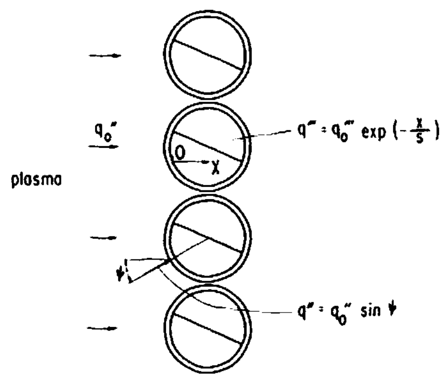

Fig. 7. Heat generation and surface heating

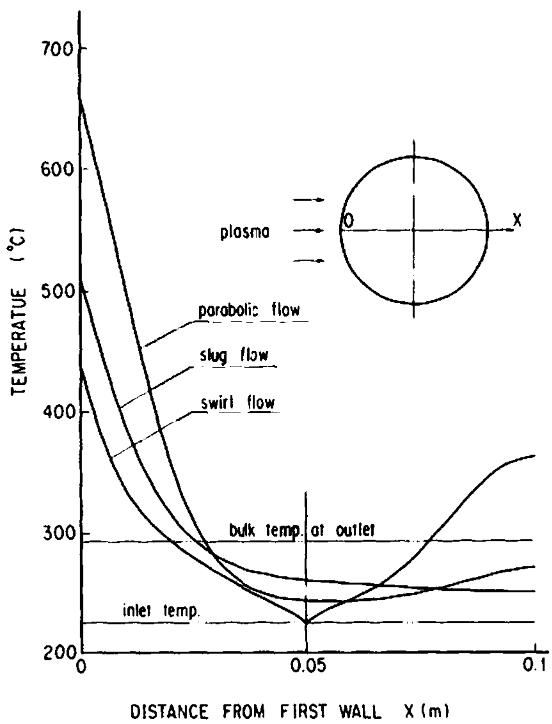

Fig. 8. Coolant temperature distribution on center line at outlet

$$q'' = q_o'' \cos \psi \qquad (67)$$

where $q_o'' = 0.75\ \mathrm{MW/m^2}$ and ψ is the incident angle of the radiant heat from the plasma. On the rear surface, the heat flux is assumed to be zero.

In addition, the following assumptions are made. The coolant temperature at the inlet is uniformly 225°C. The boundary layer is neglected. Heat conduction in the pipe wall is neglected. In the pipe with a vane, heat conduction in the vane is also neglected.

Figure 8 shows the temperature distribution at the center line of the pipe. In the case of parabolic flow, the temperature on the cooling surface of the first wall is very high. The heat transfer coefficient is low, owing to the low coolant velocity near the wall. In the case of slug flow, the temperature is lower because of a higher heat transfer coefficient.

As the coolant swirls in the pipe with a vane, the interface temperature is not highest at the point of $\psi = 0$ as might be expected. Figure 9 shows the interface temperature distribution. The difference between the maximum interface temperature and the temperature at $\psi = 0$ is not large. The maximum interface temperature is the lowest in the case of the swirl flow.

The coolant temperature at the center of the pipe with a vane does not rise at all. This is because the velocity is infinite at the center. If it is necessary to make the coolant temperature more uniform, the central part of the coolant should be eliminated. This can be attained by an

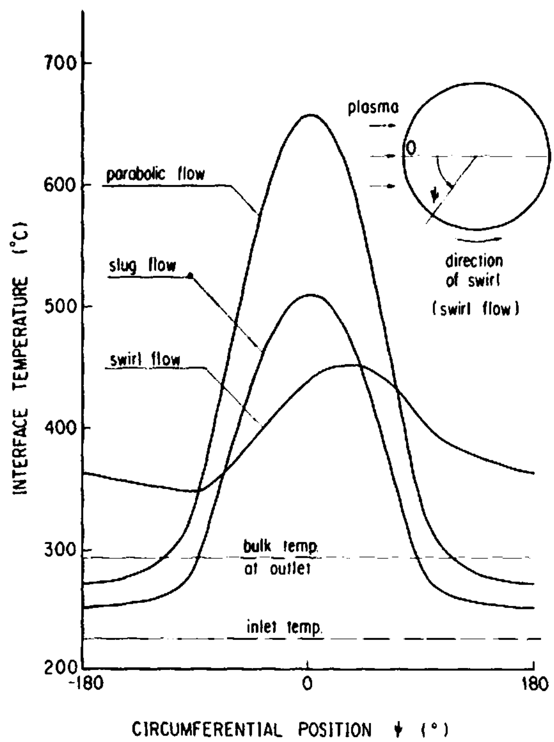

Fig. 9. Interface temperature distribution at outlet

annular channel with a turning vane shown in Fig. 10. The maximum interface temperature decreases with increasing diameter ratio d_i/d_o. This method seems attractive, but further discussion is beyond the scope of this study.

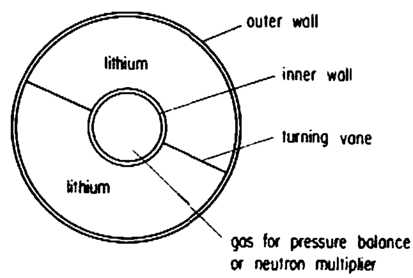

Fig. 10. Annular channel with turning vane

3.4 Discussions

From the viewpoint of pressure drop, the flow direction of the first wall cooling channel should be parallel to the magnetic field line. In this case, however, the first wall temperature is high because of the low heat transfer coefficient. When the coolant flows parallel to the magnetic field, turbulence is suppressed and the velocity profile is parabolic. From the viewpoint of first wall cooling, parabolic flow is undersirable.

When the coolant flows at an angle with the magnetic field, the electromagnetic force makes the velocity profile uniform. The heat transfer coefficient on the first wall is high because the coolant velocity is high near the wall. In this case, however, there appears an MHD pressure drop, which depends on the wall thickness of the pipe. If the pipe wall is thin, the MHD pressure drop is low. But the pipe wall must be thick enough to withstand the internal pressure. The MHD pressure drop is low if the angle between the field and flow directions is small. However, if it is too small, slug flow may not appear in the pipe.

From the viewpoint of first wall cooling, a pipe with a turning vane is very attractive. The MHD pressure drop can be reduced easily by thinning the vane. The film temperature drop is smaller than those in other cases.

Some problems relating to this concept remain. In the analysis, the flow is assumed to develop quickly. The entry region has not been examined. Inlet and outlet pipes are connected to the pipe with a vane, but detailed designs have not been made. The detailed structure of the wall jet and the Hartmann layer have not been studied. These are subjects for future study.

4. Conclusion

The flow distribution and the MHD pressure drop in a pipe with a helical vane under a strong axial magnetic field were derived analytically with the assumption of fully developed conditions. The fluid flows helically along the vane, and the velocity is almost inversely proportional to the radius. The MHD pressure drop can be reduced by thinning the vane, but the vane must be thick enough to withstand the electromagnetic load and the pressure difference on both sides of the vane.

A reference design of a liquid metal blanket with a helical vane was made. The additional pressure drop was shown to be low in the case when the vane has a reasonable thickness. The temperature distribution in the fluid was calculated and was compared with those in pipes without vanes. The vane was shown to flatten the temperature distribution with a small additional pressure drop.

References

1) Hunt, J. C. R. and Holroyd, R. J.: Applications of laboratory and theoretical MHD duct flow studies in fusion reactor technology, CLM-R169, (1977)

2) Hunt, J. C. R.: Magnetohydrodynamic flow in rectangular ducts, J. Fluid Mech., 21 (4), 577 (1965)

3) Hunt, J. C. R. and Stewartson, K.: Magnetohydrodynamic flow in rectangular ducts II, J. Fluid Mech., 23 (3), 563 (1965)